Inorganic Chemistry

Article

pubs.acs.org/IC

3-Fold-Interpenetrated Uranium−Organic Frameworks: New Strategy for Rationally Constructing Three-Dimensional Uranyl Organic Materials

Hong-Yue Wu,[†,‡] Run-Xue Wang,[†] Weiting Yang,[†] Jinlei Chen,[†] Zhong-Ming Sun,*[,†] Jun Li,[§] and Hongjie Zhang[†]

[†]State Key Laboratory of Rare Earth Resource Utilization, Changchun Institute of Applied Chemistry, Chinese Academy of Sciences, 5625 Renmin Street, Changchun, Jilin 130022, China

[‡]School of Chemistry & Environmental Engineering, Changchun University of Science & Technology, Changchun 130022, China

[§]Department of Chemistry & Key Laboratory of Organic Optoelectronics and Molecular Engineering of Ministry of Education, Tsinghua University, Beijing 100084, China

Supporting Information

ABSTRACT: The first series of 3-fold-interpenetrated uranium−organic frameworks, **UOF-1** and **UOF-2**, have been synthesized by hydrothermal reactions of flexible semirigid carboxylic acids and uranyl nitrate. Structure analyses indicate that **UOF-1** and **UOF-2** possess **flu** and **pts** topologies, respectively.

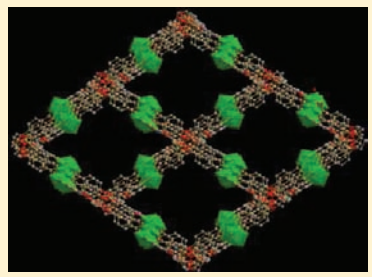

INTRODUCTION

Metal−organic frameworks (MOFs) have attracted increasing attention because of their remarkable potential applications in gas storage,[1] adsorption and separation,[2] catalysis,[3] molecule and ion sensing,[4] nonlinear optics,[5a] biomedical imaging, and drug delivery.[5b] Interpenetrated three-dimensional (3D) MOFs, compared with those low-dimensional analogies, are of particular interest because of their privilege properties, intriguing versatile architectures, and new topologies.[6] In contrast to the huge amount of transition-metal organic frameworks, 5f actinide compounds that adopt various topologies and coordination geometries have been less investigated.[7−11] Uranium, as the most representative actinide element, has been mostly investigated owing to its advantages in synthetic methods, structure diversities, and physicochemical properties for elements involved in the nuclear fuel cycle. So far, a number of typical uranium compounds with various structures have been synthesized,[9−11] such as clusters,[9] chains, layers, and 3D networks.[10,11] Among these structures, of significance are the 3D uranium−organic frameworks (UOFs) because of their superior thermal stability to one-dimensional (1D) or two-dimensional (2D) structures and outstanding properties such as photoelectronic effects,[11a] nonlinear optical properties,[11d] and porous adsorption.[11f]

In contrast to the low-dimensional compounds, even including cage clusters, the formation of 3D UOFs has proven to be less successful.[7,11] To the best of our knowledge, interpenetrated 3D UOFs have never been documented. The reason is that U^{VI} usually exists in the form of a linear O═U═O chain with a charge of 2+, namely, uranyl, leaving 4−6 coordination sites in the equatorial plane, thus favoring the formation of 1D or 2D structures. It is a challenging task to rationally design and synthesize 3D UOFs, especially the interpenetrated structures. One popular strategy to isolate 3D UOFs is introducing a second functional group such as pyridine or a carboxylate-containing moiety into the ligands, thus leaving the potential for further incorporating heterometal ions as structure-directing agents.[11a,f] Another approach is using soft aliphatic carboxylic acids or arylcarboxylic acids with strong hindrance to cross-link the inorganic uranyl moieties to form 3D networks.[11g,12] In most cases, however, it is noteworthy that linear aliphatic carboxylic acids usually form chains or sheets with uranyl cations.[13] Apart from the methods mentioned above, reaction conditions such as temperature, concentration, pH values, etc., also play significant roles in the assembly of 3D uranyl compounds.[7,14] In this paper, we describe a new strategy using semirigid carboxylic acids as organic building blocks to rationally synthesize the first examples of 3D UOFs with 3-fold-interpenetrated networks.

EXPERIMENTAL SECTION

Caution! *Standard procedures for handling radioactive material should be followed, although the uranyl nitrate hexahydrate $UO_2(NO_3)_2\cdot6H_2O$ used in the laboratory contained depleted uranium.*

Received: November 30, 2011
Published: February 10, 2012

dx.doi.org/10.1021/ic202577z | Inorg. Chem. 2012, 51, 3103−3107

Materials and Synthesis. All chemicals were purchased commercially and used without further purification: uranyl nitrate (99.8%, Sinpharm Chemical Reagent Co. Ltd.), K_2CO_3, and *N,N*-dimethylformamide (DMF; 99.5%, Jinan Henghua Sci. & Tech. Co. Ltd.). Trimethylolpropane tosylate (**C_3-OTs**) and dipentaerythrityl hexatosylate (**C_6-OTs**) were synthesized according to the literature.[15] ^{1}H and ^{13}C NMR spectra were carried out in a dimethyl sulfoxide (DMSO)-d_6 solvent on a Bruker 400 or 300 MHz spectrometer at 298 K. The chemical shifts are given in dimensionless δ values and are referenced relative to tetramethylsilane in ^{1}H and ^{13}C NMR spectroscopy. Elemental analyses of carbon, hydrogen, and nitrogen in the solid samples were performed with a VarioEL analyzer. Energy-dispersive spectroscopy spectra were obtained by using a scanning electron microscope (Hitachi S-4800) equipped with a Bruker AXS XFlash detector 4010. All IR measurements were obtained using a Bruker TENSOR 27 Fourier transform infrared spectrometer. Samples were diluted with spectroscopic KBr and pressed into a pellet. Scans were run over the range 400−4000 cm^{-1}. The fluorescence spectra were performed on a Horiba-Jobin Yvon Fluorolog-3 fluorescence spectrophotometer, equipped with a 450 W xenon lamp as the excitation source and a monochromator iHR320 equipped with a liquid-nitrogen-cooled R5509-72 photomultiplier tube as the detector.

*Synthesis of 4,4′-[[2-[(4-Carboxyphenoxy)ethyl]-2-methylpropane-1,3-diyl]dioxy]dibenzoic Acid (**H_3L^1**).* The ligand was synthesized by a modified procedure.[15,16] A mixture of **C_3-OTs** (2.00 g, 3.35 mmol), ethylparaben (2.30 g, 13.74 mmol), K_2CO_3 (1.18 g, 8.60 mmol), and 20 mL of DMF was placed in a 100-mL round-bottomed flask equipped with a magnetic stirbar. The reaction mixture was refluxed for 16 h and then cooled to room temperature. After quenching of H_2O (100 mL), the product was extracted by ethyl acetate (15 mL × 3). The volatile solvent was removed under vacuum; after chromatographic separation, to the residue was added KOH (3.85 g, 68.7 mmol), acetone (15 mL), and H_2O (25 mL), and the resulting misxture was then refluxed for 12 h. The mixture was diluted with H_2O (200 mL) and acidified by a 6 M HCl solution to pH ∼ 2.0. A white solid was precipitated and filtered. The solid was dried under vacuum. Yield: 1.21 g (2.45 mmol, 73%). ^{1}H NMR (400 MHz, DMSO-d_6): δ 12.61 (br s, 3H), 8.87 (d, J = 8.8 Hz, 6H), 7.04 (d, J = 8.8 Hz, 6H), 4.17 (s, 6H), 1.75 (m, 2H), 0.934 (t, J = 7.2 Hz, 3H). ^{13}C NMR (100 MHz, DMSO-d_6): 166.9, 162.1, 131.3, 123.2, 114.4, 67.7, 42.2, 22.6, 7.5. Elem anal. Obsd (calcd): C, 65.16 (65.58); H, 5.41 (5.30).

*Synthesis of Hexakis[4-(carboxyphenyl)oxamethyl]-3-oxapentane (**H_6L^2**).* Following a procedure similar to that of **H_3L^1**, **C_6-OTs** (2.00 g, 1.70 mmol), ethylparaben (2.26 g, 13.6 mmol), and K_2CO_3 (0.94 g, 6.80 mmol) in 20 mL of DMF were refluxed for 12 h. KOH (3.81 g, 68.0 mmol), acetone (15 mL), and H_2O (25 mL) were added, and the resulting mixture was refluxed for 12 h in the second step. Workup gave **H_6L^2** as a white solid. Yield: 1.16 g (1.19 mmol, 70%). ^{1}H NMR (300 MHz, DMSO-d_6): δ 12.40 (br s, 6H), 7.84 (d, J = 9.0 Hz, 12H), 6.95 (d, J = 9.0 Hz, 12H), 4.21 (s, 12H), 3.75 (s, 4H). ^{13}C NMR (75 MHz, DMSO-d_6): 167.4, 162.4, 131.7, 123.9, 114.7, 69.8, 67.1, 40.0 (m). Elem anal. Obsd (calcd): C, 64.39 (64.06); H, 4.37 (4.76).

*$UO_2(HL^1)$ (**UOF-1**).* The title compound was prepared by a hydrothermal method. A mixture of 0.1 M $UO_2(NO_3)_3$ aqueous solution (1.0 mL, 0.100 mmol), **H_3L^1** (57 mg, 0.1 mmol), and deionized water (5 mL, 278 mmol) was loaded into a 20-mL Teflon-lined stainless steel autoclave. The autoclave was sealed and heated at 180 °C for 3 days and then cooled to room temperature. Yellow crystals were isolated: initial pH 3.0; final pH 2.5. Yield: 42 mg (63% based on uranium). Energy-dispersive X-ray analysis of several crystals showed the presence of uranium. Elem anal. Obsd (calcd): C, 42.78 (42.53); H, 3.35 (3.17).

*$(UO_2)_3(H_2O)_2L^2$ (**UOF-2**).* To a 20-mL Teflon-lined stainless steel autoclave was added 0.1 M $UO_2(NO_3)_3$ aqueous solution (1.0 mL, 0.10 mmol), **H_6L^2** (60 mg, 0.062 mmol), and deionized water (5 mL, 278 mmol). The mixture was heated at 180 °C for 7 days and then cooled to room temperature. Yellow platelets of the title compound suitable for single-crystal X-ray diffraction studies were isolated: initial pH 3.0; final pH 2.3. Yield: 102 mg (56% based on uranium). Energy-dispersive X-ray analysis of several crystals showed the presence of uranium. Elem anal. Obsd (calcd): C, 34.65 (34.49); H, 2.31 (2.23).

X-ray Crystal Structure Determination. Suitable single crystals with dimensions of 0.24 × 0.32 × 0.08 mm^3 for **1** and 0.18 × 0.26 × 0.06 mm^3 for **2** were selected for single-crystal X-ray diffraction analyses. Crystallographic data were collected at 293 K on a Bruker Apex II CCD diffractometer with graphite-monochromated Mo Kα radiation (λ = 0.710 73 Å). Data processing was accomplished with the *SAINT* program. The structures were solved by direct methods and refined on F^2 by full-matrix least squares using *SHELXTL-97*.[17] Non-hydrogen atoms were refined with anisotropic displacement parameters during the final cycles. All hydrogen atoms of the organic molecule were placed by geometrical considerations and were added to the structure factor calculation. A summary of the crystallographic data for these two complexes is listed in Table 1. Selected bond distances and angles are given in Tables 2 and 3.

■ RESULTS AND DISCUSSION

In our understanding, ligands with flexible backbones combining rigid multicoordination sites are good building blocks to

Table 1. Crystallographic Data for UOF-1 and UOF-2

	UOF-1	UOF-2
fw	762.49	1810.93
space group	C2/*c* (No. 15)	
a/Å	26.1023(19)	35.621(3)
b/Å	9.6889(7)	9.2925(8)
c/Å	23.6885(17)	20.4260(17)
β/deg	93.1170(10)	114.6560(10)
V/Å^3	5982.0(7)	6144.7(9)
Z	8	4
T/K	293(2)	
λ(Mo Kα)/Å	0.710 73	
ρ_{calcd}/(g cm^{-3})	1.693	1.958
μ(Mo Kα)/mm^{-1}	5.481	7.968
GOF	1.015	1.047
R1/wR2 [$I > 2\sigma(I)$]^a	0.0347/0.0687	0.0468/0.1275
R1/wR2 (all data)	0.0600/0.0758	0.0799/0.1496

^{a}R1 = $\sum||F_o| - |F_c||/\sum|F_o|$, wR2 = $\{\sum w[(F_o)^2 - (F_c)^2]^2/\sum w[(F_o)^2]^2\}^{1/2}$.

Table 2. Selected Bond Lengths and Bond Angles for UOF-1^a

U1−O1	1.722(4)	U1−O2	1.741(4)
U1−O4#1	2.283(3)	U1−O3	2.310(3)
U1−O5#2	2.428(4)	U1−O8#3	2.443(4)
U1−O7#3	2.468(3)		
O1−U1−O2	179.24(17)	O2−U1−O8#3	88.94(17)
O1−U1−O4#1	90.56(15)	O4#1−U1−O8#3	128.94(12)
O2−U1−O4#1	89.85(16)	O3−U1−O8#3	145.71(12)
O1−U1−O3	89.08(15)	O5#2−U1−O8#3	68.94(12)
O2−U1−O3	91.58(16)	O1−U1−O7#3	88.58(15)
O4#1−U1−O3	85.35(12)	O2−U1−O7#3	90.90(16)
O1−U1−O5#2	88.72(16)	O4#1−U1−O7#3	76.54(12)
O2−U1−O5#2	91.08(17)	O3−U1−O7#3	161.71(12)
O4#1−U1−O5#2	162.12(12)	O5#2−U1−O7#3	121.30(12)
O3−U1−O5#2	76.77(12)	O8#3−U1−O7#3	52.45(12)
O1−U1−O8#3	90.31(16)		

^{a}Symmetry code: #1, $-x + 1, -y - 1, -z$; #2, $-x + 1, y, -z + {}^1/_2$; #3, $x - {}^1/_2, y - {}^3/_2, z$.

Table 3. Selected Bond Lengths and Bond Angles for UOF-2[a]

U1−O12	1.689(10)	U1−O11	1.746(8)
U1−O8	2.297(7)	U1−O9#1	2.317(7)
U1−O6#2	2.426(8)	U1−O5#2	2.427(8)
U1−O1W	2.462(9)	U2−O13	1.739(8)
U2−O10#1	2.276(8)	U2−O7	2.287(7)
O12−U1−O11	178.8(5)	O12−U1−O1W	89.1(5)
O12−U1−O8	90.2(4)	O11−U1−O1W	89.8(4)
O11−U1−O8	91.0(3)	O8−U1−O1W	161.0(3)
O12−U1−O9#1	90.9(4)	O9#1−U1−O1W	76.2(3)
O11−U1−O9#1	89.4(3)	O6#2−U1−O1W	121.8(3)
O8−U1−O9#1	84.9(3)	O5#2−U1−O1W	68.8(3)
O12−U1−O6#2	90.6(4)	O13−U2−O13#3	180.0
O11−U1−O6#2	89.5(4)	O13−U2−O10#1	90.0(4)
O8−U1−O6#2	77.2(3)	O10#1−U2−O10#4	180.0
O9#1−U1−O6#2	162.0(3)	O13−U2−O7	88.3(4)
O12−U1−O5#2	89.3(4)	O13#3−U2−O7	91.7(4)
O11−U1−O5#2	89.8(4)	O10#1−U2−O7	89.0(3)
O8−U1−O5#2	130.2(3)	O10#4−U2−O7	91.0(3)
O9#1−U1−O5#2	144.9(3)	O7−U2−O7#3	180.0(2)
O6#2−U1−O5#2	53.0(3)		

[a]Symmetry code: #1, $x, -y, z + {}^{1}/_{2}$; #2, $-x + {}^{1}/_{2}, -y + {}^{3}/_{2}, -z + 2$; #3, $-x, -y, -z + 2$; #4, $-x, y, -z + {}^{3}/_{2}$.

construct new 3D uranyl coordination polymers. On the basis of this point, semirigid carboxylic acids **H_3L^1** and **H_6L^2** (Scheme 1) are adopted in this work, clearly their versatile

Scheme 1. Structures of Ligands H_3L^1 and H_6L^2

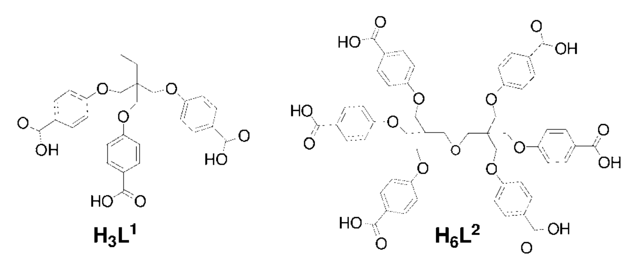

coordination directions in space make the design and prediction of the 3D networks possible. Hydrothermal reactions of **H_3L^1**, **H_6L^2**, and $UO_2(NO_3)_2{\cdot}6H_2O$ at 180 °C resulted in compounds **UOF-1** and **UOF-2**, respectively. Single-crystal X-ray diffraction studies indicate that both compounds adopt the same monoclinic space group *C*2/*c* but are not isostructural (Table 1).

As shown in Figure 1a, the asymmetric unit of **UOF-1** consists of one uranyl unit and one protonated L^1 ligand. The uranium atom is seven-coordinated by oxygen atoms, resulting in a pentagonal bipyramid as the primary building unit. Axially, the O═U═O angle is 179.24(17)°, and the U═O lengths are 1.722(4) and 1.741(4) Å. Equatorially, the uranium atom is five-coordinated to μ_2-oxygen atoms from the carboxylate groups of three L^1 ligands [U−O, 2.283(3)−2.468(3) Å]. In order to keep a charge balance, L^1 is protonated at the O6 site [C14−O6, 1.320(6) Å]. The asymmetric unit of **UOF-2** (Figure 1b) contains one and a half crystallographically independent uranyl units and half of a L^2 ligand. The U1 atom exists in the form of a UO_7 pentagonal bipyramid including two linear uranyl oxygen atoms [O═U═O, 178.8(5)°; U═O, 1.689(10) and 1.746(8) Å], four planar μ_2-oxygen atoms from three L^2 ligands [U−O, 2.297(7)−2.427(8) Å], and one aqua ligand [U−O, 2.462(9) Å], while the U2 atom is octahedrally coordinated to four μ_2-oxygen atoms shared with four adjacent carboxylate groups from four L^2 ligands [U−O, 2.276(8)−2.287(7) Å], leaving two axial oxygen atoms to form a uranyl unit [O═U═O, 180°; U═O, 1.739(8) Å]. These values are within the typical bond length ranges reported for uranium-containing materials. Selected bond lengths and angles are listed in Tables 2 and 3.

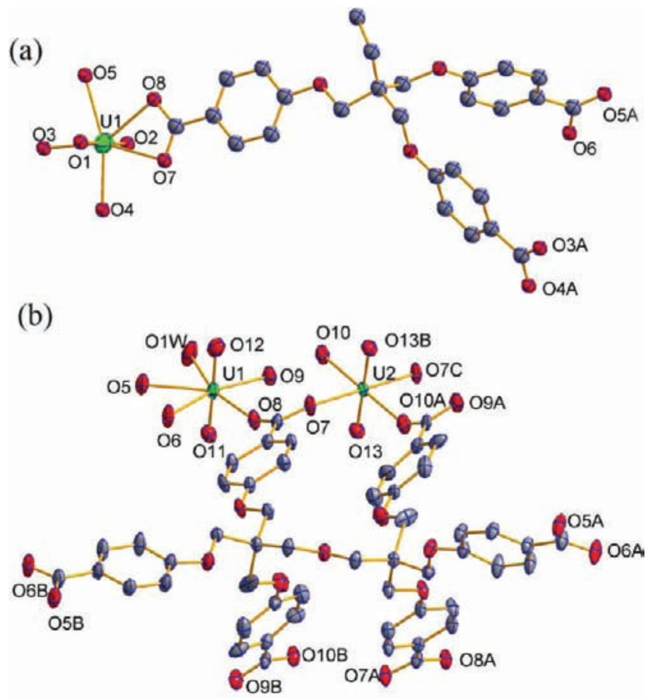

Figure 1. ORTEP representation of the asymmetric units of **UOF-1** (a) and **UOF-2** (b). Thermal ellipsoids are drawn at the 30% probability level, and the hydrogen atoms are omitted for clarity. Symmetry codes for **UOF-1**: A, 0.5 − *x*, 0.5 + *y*, 0.5 − *z*. Symmetry codes for **UOF-2**: A, 0.5 + *x*, 0.5 + *y*, *z*; B, 0.5 − *x*, 0.5 + *y*, 0.5 − *z*; C, 0.5 + *x*, 0.5 − *y*, −0.5 + *z*.

The most striking features of **UOF-1** and **UOF-2** are the connections between UO_2^{2+} and the ligands to form 3D interpenetrated networks. In **UOF-1**, the structure adopts a dimeric uranyl unit as its secondary building unit (SBU; Figure 2a), which is further linked by L^1 to form a 3D network with large parallelogram channels along the ⟨111⟩ direction, in which the diagonal lengths are around 20.2 and 35.5 Å and the bent angle is 58.5°. Similarly, the single net in **UOF-2** also exhibits a porous 3D framework with large channels but adopts trimeric uranyl units (including one square bipyramid and two pentagonal bipyramids) as its SBUs (Figure 2b). The diagonal lengths within the channels are around 20.4 and 34.8 Å and the bent angle is 60.5°. Because of the large void volume of the single nets in **UOF-1** and **UOF-2**, triple equivalent networks interpenetrate each other to keep their stabilities of the whole structure. The space-filling models in Figure 3 clearly display this feature; each net is represented by a unique color, including red, green, and blue. Simplified interpenetrating srtuctures are shown in Figure 4. On the basis of the calculations using the *PLATON* program,[18] the total potential solvent-accessible void volumes (pore volume ratio) per unit cell are ~801.6 Å^3

dx.doi.org/10.1021/ic202577z | Inorg. Chem. 2012, 51, 3103−3107

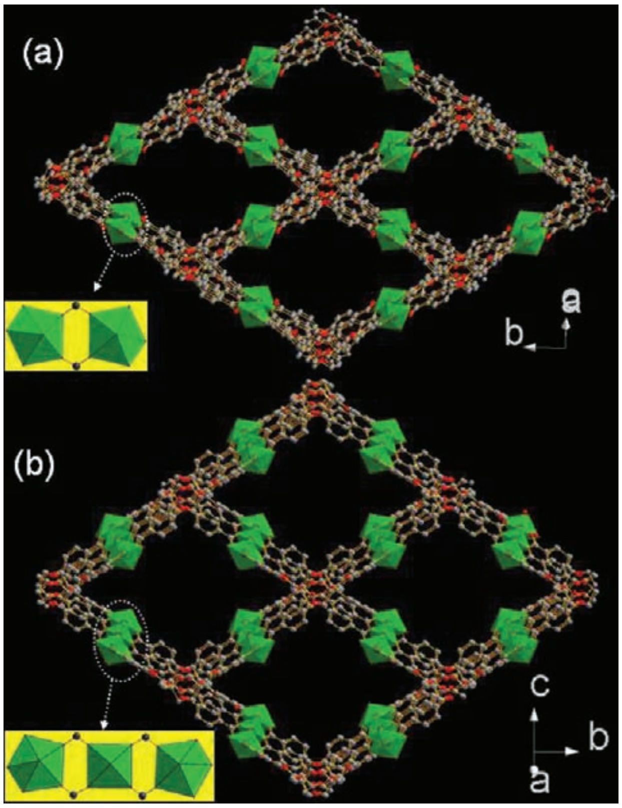

Figure 2. Single net views of **UOF-1** (a) and **UOF-2** (b). The SBUs are shown on the bottom left.

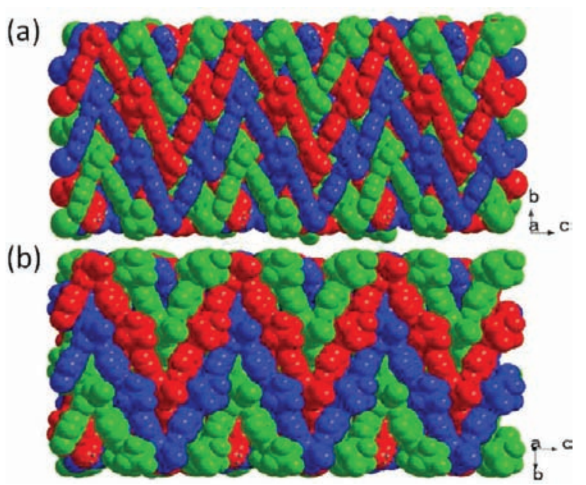

Figure 3. Space-filling model of 3D networks in **UOF-1** (a) and **UOF-2** (b). The nets are depicted by different colors: red, green, and blue.

(13.4%) and 1020.0 Å^3 (16.6%) for **UOF-1** and **UOF-2**, respectively.

To further understand the complicated structures, topological analyses were employed.[19] In **UOF-1**, every uranyl SBU is surrounded by six L^1 units, and each L^1 linker connects three uranyl SBUs to form a 3D framework. The uranyl SBU and L^1 ligand can be considered as 6- and 3-connected nodes, respectively. Thus, **UOF-1** can be represented as a 3,6-connected 3-fold-interpenetrating net with a Schlafli symbol of $(4^2.6)_2(4^4.6^2.8^7.10^2)$ and **flu**-3,6-*C*2/*c* topology (Figure 4b). Accordingly, every uranyl SBU in **UOF-2** is surrounded by four L^2 ligands, and each L^2 linker also connects four uranyl SBUs to form the framework. As a result, the underlying topology of the compound is a 4-connected net with both the center of the uranyl SBU and the center of the L^2 unit as nodes. Topological analysis indicates that **UOF-2** adopts a **pts** net with a Schlfli symbol of $(4^2.8^4)$ (Figure 4d).

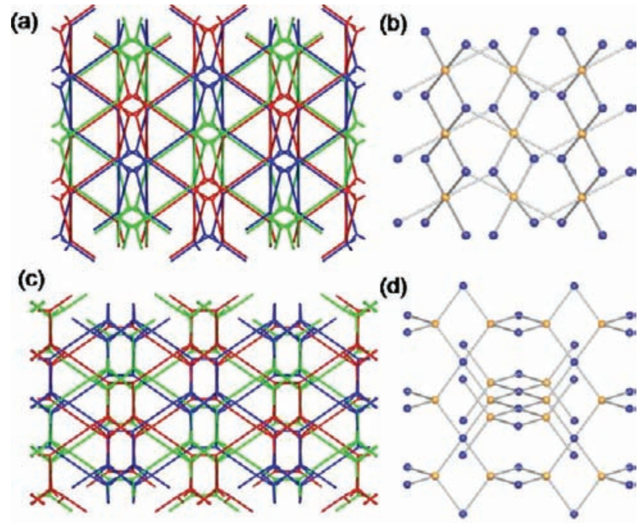

Figure 4. Simplified 3-fold-interpenetrated networks of **UOF-1** (a) and **UOF-2** (c) colored separately in red, green, and blue. Topological presentations of **UOF-1** (b) and **UOF-2** (d).

The IR spectra of **UOF-1**, **UOF-2**, $\mathbf{H_3L^1}$, and $\mathbf{H_6L^2}$ are shown in Figure 5. The spectra of **UOF-1** and **UOF-2** exhibit additional vibrational peaks around 950 and 880 cm^{-1} compared to the ligands, which are attributed to the asymmetric and symmetric U═O vibrations, respectively (934 and 878 cm^{-1} for **UOF-1**; 954 and 878 cm^{-1} for **UOF-2**). In **UOF-2**, the stretching vibration of the coordinated H_2O molecule is clearly indicated on a broad band centered at 3448 cm^{-1}.

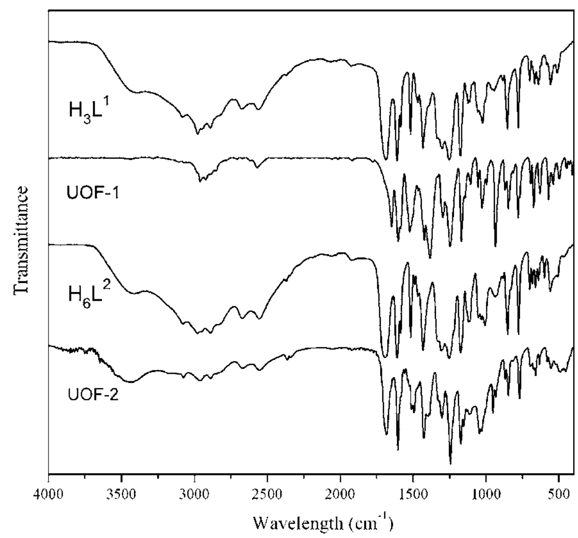

Figure 5. IR spectra of **UOF-1**, **UOF-2**, and the ligands $\mathbf{H_3L^1}$ and $\mathbf{H_6L^2}$.

The photoluminescent properties of **UOF-1** and **UOF-2** were characterized, and only emission of the ligands was observed instead of the characteristic emission features of UO_2^{2+}. This implies that the UO_2^{2+}-centered luminescence is poorly sensitized by the ligands.

In conclusion, two new 3D uranium organic frameworks have been hydrothermally synthesized using uranyl cations and semirigid carboxylic acids with flexible backbones; both compounds feature 3-fold-interpenetrated structures. This method provides a new strategy to rationally design and synthesize new uranium–organic compounds. Future work will be focused on the syntheses of further extended structures of 3D UOFs using secondary ligands, which may result in micro/mesoporous materials with potential applications in gas separation or absorption.

■ ASSOCIATED CONTENT

Ⓢ Supporting Information

X-ray crystallographic CIF file. This material is available free of charge via the Internet at http://pubs.acs.org.

■ AUTHOR INFORMATION

Corresponding Author

*E-mail: szm@ciac.jl.cn.

Notes

The authors declare no competing financial interest.

■ ACKNOWLEDGMENTS

This work was supported by the National Nature Science Foundation of China (Grant 21171662) and CIAC startup fund. W.Y. is thankful for support of the China Postdoctoral Science Foundation (CPSF No. 20110491327).

■ REFERENCES

(1) (a) Dinca, M.; Long, J. R. *Angew. Chem., Int. Ed.* **2008**, *47*, 6766–6779. (b) Rowsell, J. L. C.; Yaghi, O. M. *Angew. Chem., Int. Ed.* **2005**, *44*, 4670–4679.

(2) (a) Liu, Y.; Xuan, W. M.; Cui, Y. *Adv. Mater.* **2010**, *22*, 4112–4135. (b) Li, J. R.; Kuppler, R. J.; Zhou, H. C. *Chem. Soc. Rev.* **2009**, *38*, 1477–1504.

(3) (a) Lee, J.; Farha, O. K.; Roberts, J.; Scheidt, K. A.; Nguyen, S. T.; Hupp, J. T. *Chem. Soc. Rev.* **2009**, *38*, 1450–1459. (b) Ma, L. Q.; Abney, C.; Lin, W. B. *Chem. Soc. Rev.* **2009**, *38*, 1248–1256. (c) Ma, L. Q.; Falkowski, J. M.; Abney, C.; Lin, W. B. *Nat. Chem.* **2010**, *2*, 838–846.

(4) (a) Chen, B.; Xiang, S.; Qiang, G. *Acc. Chem. Res.* **2010**, *43*, 1115–1124. (b) Xie, Z. G.; Ma, L. Q.; Dekrafft, K. E.; Jin, A.; Lin, W. B. *J. Am. Chem. Soc.* **2010**, *132*, 922–923.

(5) (a) Evans, O. R.; Lin, W. B. *Acc. Chem. Res.* **2002**, *35*, 511–522. (b) Liu, D.; Lin, W. B. *Acc. Chem. Res.* **2011**, DOI: 10.1021/ar200028a

(6) (a) Carlucci, L.; Ciani, G.; Proserpio, D. M. *Coord. Chem. Rev.* **2003**, *246*, 247–289. (b) Wu, H.; Yang, J.; Su, Z. M.; Batten, S. R.; Ma, J. F. *J. Am. Chem. Soc.* **2011**, *133*, 11406–11409.

(7) For a recent review on uranium–organic compounds, see: Wang, K. X.; Chen, J. S. *Acc. Chem. Res.* **2011**, *44*, 531–540.

(8) (a) Kim, J. Y.; Norquist, A. J.; O'Hare, D. *J. Am. Chem. Soc.* **2003**, *125*, 12688. (b) Ok, K. M.; Sung, J.; Hu, G.; Jacobs, R. M. J.; O'Hare, D. *J. Am. Chem. Soc.* **2008**, *130*, 3762–3763.

(9) (a) Burns, P. C. *Can. Mineral.* **2005**, *43*, 1839–1894. (b) Forbes, T. Z.; McAlpin, J. G.; Murphy, R.; Burns, P. C. *Angew. Chem., Int. Ed.* **2008**, *47*, 2824. (c) Ling, J.; Qiu, J.; Sigmon, G. E.; Ward, M.; Szymanowski, J. E. S.; Burns, P. C. *J. Am. Chem. Soc.* **2010**, *132*, 13395. (d) Ling, J.; Wallace, C. M.; Szymanowski, J. E. S.; Burns, P. C. *Angew. Chem., Int. Ed.* **2010**, *49*, 7271. (e) Sigmon, G. E.; Burns, P. C. *J. Am. Chem. Soc.* **2011**, *133*, 9137–9139.

(10) (a) Liao, Z. L.; Li, G. D.; Bi, M. H.; Chen, J. S. *Inorg. Chem.* **2008**, *47*, 4844–4853. (b) Zheng, Y. Z.; Tong, M. L.; Chen, X. M. *Eur. J. Inorg. Chem.* **2005**, 4109–4117.

(11) For selected 3D examples, see: (a) Chen, W.; Yuan, H. M.; Wang, J. Y.; Liu, Z. Y.; Xu, J. J.; Yang, M.; Chen, J. S. *J. Am. Chem. Soc.* **2003**, *125*, 9266–9267. (b) Adelani, P. O.; Albrecht-Schmitt, T. E. *Angew. Chem., Int. Ed.* **2010**, *49*, 8909–8911. (c) Wang, S.; Alekseev, E. V.; Diwu, J.; Casey, W. H.; Phillips, B. L.; Depmeier, W.; Albrecht-Schmitt, T. E. *Angew. Chem., Int. Ed.* **2010**, *49*, 1057. (d) Wang, S.; Alekseev, E. V.; Ling, J.; Liu, G.; Depmeier, W.; Albrecht-Schmitt, T. E. *Chem. Mater.* **2010**, *22*, 2155. (e) Sykora, R. E.; King, J.; Illies, A.; Albrecht-Schmitt, T. E. *J. Solid State Chem.* **2004**, *177*, 1717. (f) Alsobrook, A. N.; Hauser, B. G.; Hupp, J. T.; Alekseev, E. V.; Depmeierc, W.; Albrecht-Schmitt, T. E. *Chem. Commun.* **2010**, *46*, 9167–9169. (g) Liao, Z. L.; Li, G. D.; Wei, X.; Yu, Y.; Chen, J. S. *Eur. J. Inorg. Chem.* **2010**, 3780–3788.

(12) (a) Thuéry, P. *Chem. Commun.* **2006**, 853–855. (b) Thuéry, P. *Polyhedron* **2006**, *27*, 101–106.

(13) (a) Borkowski, L. A.; Cahill, C. L. *Cryst. Growth Des.* **2006**, *10*, 2241–2247. (b) Borkowski, L. A.; Cahill, C. L. *Cryst. Growth Des.* **2006**, *10*, 2248–2259. (c) Kerr, A. T.; Cahill, C. L. *Cryst. Growth Des.* **2011**, DOI: 10.1021/cg2011869.

(14) Walker, S. M.; Halasyamani, P. S.; Allen, S.; O'Hare, D. *J. Am. Chem. Soc.* **1999**, *121*, 10513.

(15) Keegstra, E. M. D.; Zwikker, J. W.; Roest, M. R.; Jenneskens, L. W. *J. Org. Chem.* **1992**, *57*, 6678.

(16) (a) Wang, Y. W.; Zhang, Y. L.; Dou, W.; Zhang, A. J.; Qin, W. W.; Liu, W. S. *Dalton Trans.* **2010**, *39*, 9013. (b) Laliberte, D.; Maris, T.; Sirois, A.; Wuest, J. D. *Org. Lett.* **2003**, *5*, 4787. (c) Laliberte, D.; Maris, T.; Wuest, J. D. *J. Org. Chem.* **2004**, *69*, 1776.

(17) Sheldrick, G. M. *Acta Crystallogr., Sect. A: Found. Crystallogr.* **2008**, *64*, 112.

(18) Spek, A. L. *J. Appl. Crystallogr.* **2003**, *36*, 7.

(19) (a) Blatov, V. A.; Shevchenko, A. P.; Serezhkin, V. N. *Acta Crystallogr., Sect. A* **1995**, *51*, 909. (b) Blatov, V. A.; Carlucci, L.; Ciani, G.; Proserpio, D. M. *CrystEngComm* **2004**, *6*, 378.